Low In solubility and band offsets in the small-x β-$\mathbf{Ga_2O_3}$/$\mathbf{(Ga_{1-x}In_x)_2O_3}$ system

Maria Barbara Maccioni, Francesco Ricci, and Vincenzo Fiorentini

Department of Physics, University of Cagliari, and CNR-IOM,
UOS Cagliari, Cittadella Universitaria, 09042 Monserrato (CA), Italy

Based on first-principles calculations, we show that the maximum reachable concentration x in the $(Ga_{1-x}In_x)_2O_3$ alloy in the low-x regime (i.e. In solubility in β-Ga_2O_3) is around 10%. We then calculate the band alignment at the (100) interface between β-Ga_2O_3 and $(Ga_{1-x}In_x)_2O_3$ at 12%, the nearest computationally treatable concentration. The alignment is strongly strain-dependent: it is of type-B staggered when the alloy is epitaxial on Ga_2O_3, and type-A straddling in a free-standing superlattice. Our results suggest a limited range of applicability of low-In-content GaInO alloys.

The wide-band gap and large-breakdown-voltage insulator Ga_2O_3 is attracting interest for high-power transport, transparent electronics, and ultraviolet sensing applications. Combined with In_2O_3 (already widely used as transparent conducting oxide), Ga_2O_3 may originate a new $(Ga_{1-x}In_x)_2O_3$ materials system enabling the band-engineering and nanostructuration concepts from popular semiconductor systems (such as, e.g., arsenides and nitrides) in a previously impervious region of high absorption energies and breakdown voltages. In this Letter we provide two key pieces of information for this endeavor, namely the maximum concentration of indium in the alloy and the interface band offset, which are hitherto unknown to our knowledge.

We first address the degree of miscibility of Ga_2O_3 and In_2O_3. The parent materials have different structures (monoclinic β and cubic bixbyite, respectively), so the low-In and high-In-content alloying limits will be different, with likely complicated phase mixing at intermediate concentrations [1, 2]. Here we consider the alloying of β-Ga_2O_3 with In, and show, based on ab initio calculations, that In can be incorporated into β-Ga_2O_3 at most at the 10% level at typical growth temperatures. This agrees with the most recent estimate [2] of around 10%. We then address the band offsets at the (100) interface of β-Ga_2O_3 to the $(Ga_{1-x}In_x)_2O_3$ alloy, both epitaxial on Ga_2O_3 and free-standing. Given that x is at most around 10%, we study the offset in the computationally-affordable case of 12% In. We find that the alignment is of type-B staggered when the alloy is epitaxial on Ga_2O_3, and type-A straddling in a free-standing superlattice.

Alloying of monoclinic β-Ga_2O_3, the stable phase at ambient condition [3], is simulated by substituting Ga with In at various nominal concentrations and configurations. The interface is then simulated by a superlattice supercell. All optimizations (internal geometry, volume, etc.) and electronic structure calculations are done within density functional theory (DFT) in the generalized gradient approximation (GGA), and the projector-augmented wave (PAW) method as implemented in the VASP code [4]. The PAWs include occupied d states in the valence for both cations. For the alloy calcula-

tion we use an 80-atom (32-cation) supercell containing 1×4×1 20-atom conventional cells, and for the interface calculation a 160-atom (32-cation) 2×2×2 supercell. The k-point sampling is on a 2×4×2 grid. We work at the calculated lattice parameters a=12.46 Å, b=3.08 Å, c=5.88 Å, θ=103.65°, which compare well with experiment [5, 6].

We choose as dilute limit the concentration of 3% In, i.e. one "isolated" In atom per 80-atom cell. Besides being computational feasible, 3% is actually a quantitatively accurate dilute limit: the formation energy calculated in the standard way [7] is $E_f(1)$=0.24 eV/In, which yields a concentration of 2.7% at the typical growth temperature T_g=775÷800 K [1, 2]. The chemical-potential reservoir for In is the bixbyite phase of In_2O_3, which might occur in nanograins embedded in Ga_2O_3.
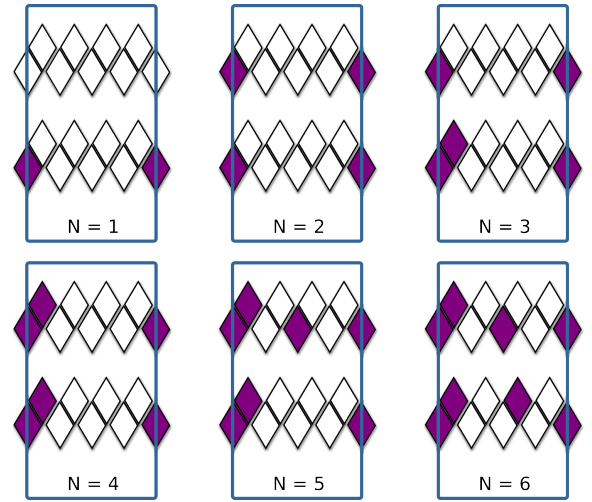

FIG. 1. (Color online) Sketch of different configurations of In on the Ga_2O_3 simulation supercell. Occupied octahedra in the β structure double-rows are darkened.

Indium substitution at tetrahedral sites costs δE_t=1.1 eV more than at octahedral sites; thus the tetrahedral-site occupation probability is lower than that of octa-

hedral sites by a factor $\exp{(-\delta E_t/k_B T_g)}{\sim}0.5\text{-}1{\times}10^{-7}$. Therefore, the In concentration in Ga_2O_3 cannot exceed the value whereby the octahedral sites are all occupied, i.e. 50%. Because the Ga_2O_3 structure is made up of double rows of octahedra sharing sides and connected by tetrahedra, there is limited configurational lee-way for In placement in the system (see Fig.1; for a more realistic depiction see e.g. Ref.[6]). We evaluate the energetics of In substitution in various configurations (a sample is depicted in Fig.1) at concentrations between 6% and 25%, i.e. for 2 to 8 In atoms in the 80-atom, 32-cation $1{\times}4{\times}1$ cell, and extrapolate numerically to 16 atoms per cell (tetrahedral sites are neglected). We find that two In's prefer to sit on different double-rows or, failing that (as inevitably is the case for growing x), on first-neighbor octahedra in adjacent subrows, which locally resemble the native In_2O_3 bixbyite structure. The formation energy per In decreases slightly for two and three In per cell, then increases steadily. For the configurations in Fig.1 we find that the excess formation energies over that of a single In are $\delta E_f(2){=}{-}0.044$, $\delta E_f(3){=}{-}0.019$, $\delta E_f(4){=}{+}0.021$, $\delta E_f(5){=}{+}0.074$, $\delta E_f(6){=}{+}0.144$, $\delta E_f(7){=}{+}0.171$, $\delta E_f(8){=}{+}0.180$, in eV/In (the last two are not shown in the Figure). The cell is kept at the volume of the undoped material, which is strictly correct in the dilute limit [8]; at higher concentration we account for an enthalpic energy cost (see below). The concentration is evaluated as the thermal average of the In population in the supercell ($M{=}32$ cation sites)

$$x = \frac{\langle N \rangle}{M} = \frac{1}{M} \frac{\sum_{N=1}^{M} N \exp{[-\beta_g F(N)]}}{\sum_{N=1}^{M} \exp{[-\beta_g F(N)]}}, \qquad (1)$$

where $\beta_g{=}1/k_B T_g$ and $F(N){=}E_f(1){+}\delta E_f(N){-}T_g S{+}\delta H$ is the free energy per In in the N-In substituted cell. E is the formation energy, S the formation vibrational entropy (we estimate it from the Debye temperature of the two bulk oxides, and find $T_g S{\simeq}0.015$ eV), and $\delta H{\simeq}0.09$ eV is the energy cost related to the internal pressure building up in the constrained cell. δH is estimated as the energy difference (per In) between the constrained and volume-relaxed cell; if cell-length changes are allowed along a given direction, as would occur in epitaxy, δH decreases by about one third. In any event, as we have seen, entropy and enthalpy provide only small corrections over the structural energy E_f discussed above. The thermal population average, Eq.1, gives a concentration of 9%, with an error bar of +2% and –1% estimated varying the δE's between 0.5 and 1.5 times those calculated. Again, this low solubility follows from tetrahedral sites being ruled out and from In occupying only about 3 out of 16 octahedral sites in the cell on (thermal) average.

Having established the small solubility of In in Ga_2O_3, we come to the band offsets. The correct way of calculating band offsets [9] is as the sum $\Delta E_b{+}\Delta V$ of the interface jump ΔV in electrostatic potential between the two regions being interfaced, and the difference ΔE_b of the band edge of interest in each of the two materials, taken separately each in their own internal potential. As mentioned, we use a $2{\times}2{\times}2$ 160-atom cell, depicted in Fig.2, upper panel, to describe the (100) interface: half of the supercell along the (100) axis is pure Ga_2O_3, and the other half is a Ga-In alloy. We pick the concentration of 12% as it is near the maximum achievable (as discussed previously), and because, given the energetics constraints, the configurational freedom of In is very limited, and there is no serious need for a detailed In configurations sampling, which would be computationally unfeasible. We choose the (100) interface for computational convenience; it remains to be assessed how much the offsets change with orientation.
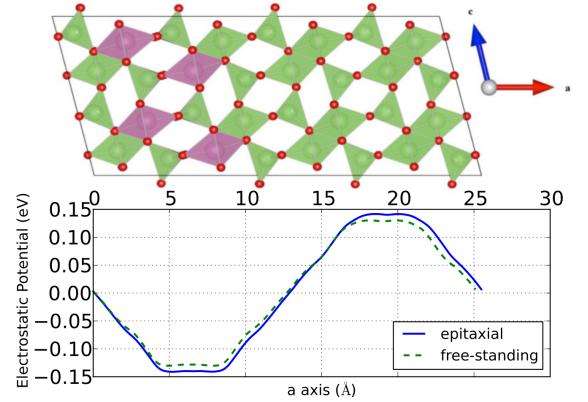

FIG. 2. (Color online) Upper panel: simulation cell for the (100) superlattice (for definiteness we display the epitaxial geometry). Lower panel: the electrostatic potential of the superlattice, showing small but definite bulk regions on either side of the interface. The potential is aligned with the lower side of the cell.

This super-unit cell repeats periodically the two layers, effectively producing a superlattice; we find that the thickness of the layers is sufficient to reproduce identifiable bulk regions on either side of interface, with flat, bulk-like average potential, as shown in Fig.2, lower panel. We study this superlattice in two strain states, epitaxial and free-standing; in the former case we fix the lattice constants in the b-c crystal plane and the monoclinic angle to those of Ga_2O_3, and relax the a lattice parameter; in the second case, we optimize all lattice parameters. The internal coordinates are optimized in all cases.

As schematized in Fig.3, at the (100) interface between Ga oxide and the alloy at 12% In, we find an alignment of type-B staggered when the alloy is epitaxial on Ga_2O_3, and type-A straddling in a free-standing superlattice; the valence offsets from Ga_2O_3 to $(Ga_{1-x}In_x)_2O_3$ are –0.14 eV (Ga_2O_3-epitaxial) and 0.15 eV (free-standing), and the conduction offsets are –0.41 eV (epitaxial) and
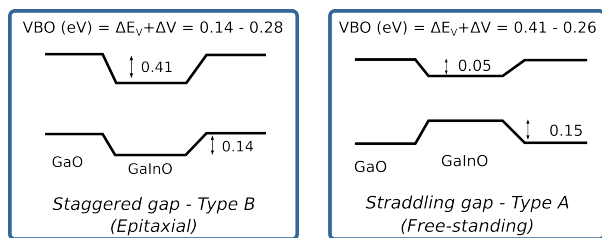
FIG. 3. (Color online) Schematic of the staggered and straddling offset for, respectively, the epitaxial and free-standing superlattice configurations.

–0.05 eV (free-standing). This considerable difference is due almost entirely to strain-induced shifts of the valence band maximum (VBM) and conduction band minimum (CBM), whereas the electrostatic interface alignment is hardly insensitive to strain. This indicates that a marked dependence on the strain state, and hence on the growth quality, is to be expected. Importantly, given the limited In solubility, this is about as much of an offset as can be expected between Ga_2O_3 and $(Ga_{1-x}In_x)_2O_3$. There seems to be no measurement of the quantities just discussed, and we hope our prediction will stimulate work in this direction.

We expect the above estimate to be rather accurate. Our interface is between materials differing only very slightly due to compositional changes, so that beyond-DFT corrections to the band edges will essentially cancel out; on the other hand, strain-induced band-edge shifts are known to be well described by standard functionals [10]. By the same token, in this case, the gap error also essentially cancels out, so the absolute value of the gap is immaterial to the offsets. For completeness, we mention that the GGA gap is about 2 eV, i.e., as expected, a 60% underestimate compared to experiment [1, 11]. Adding an empirical self-energy correction [12] involving the calculated high-frequency dielectric constant, we obtain a gap of 4.2 eV, not far from the most recent experimental and theoretical beyond-DFT estimates of 4.6 and 4.7 eV, respectively, to be discussed elsewhere [11]. As reported previously [6], the gap rates of change with composition and volume are also close to experiment [1].

In summary, we have performed first-principles calculations on the bulk and interface properties of the $Ga_2O_3/$ $(Ga_{1-x}In_x)$ system. Importantly, we find that

In is soluble in Ga_2O_3 only up to a maximum of about 10%. The band offset between Ga oxide and the alloy at 12% In is of type-B staggered when the alloy is epitaxial on Ga_2O_3, and type-A straddling in a free-standing superlattice. The valence offsets from Ga_2O_3 to $(Ga_{1-x}In_x)_2O_3$ are –0.14 eV (Ga_2O_3-epitaxial) and 0.15 eV (free-standing), and the conduction offsets are –0.41 eV (epitaxial) and –0.05 eV (free-standing).

[1] F. Zhang, K. Saito, T. Tanaka, M. Nishio, and Q. Guo, Solid State Comm. **186**, 28 (2014).
[2] M. Baldini, D. Gogova, K. Irmscher, M. Schmidbauer, G. Wagner, and R. Fornari, Cryst. Res. Technol. **49**, 552 (2014)
[3] D. F. Edwards, *Handbook of Optical Constants of Solids* (Academic Press, New York 1998), p. 753, vol. III.
[4] G. Kresse and J. Furthmuller Phys. Rev. B **54**, 11169 (1996).
[5] S. Geller, J. Chem. Phys. **33**, 676 (1960).
[6] M. B. Maccioni, F. Ricci, and V. Fiorentini, J. Phys Conf. Ser., in print (2014).
[7] D. B. Laks, C. G. Van de Walle, G. F. Neumark, P. E. Blöchl, and S. T. Pantelides, Phys. Rev. B **45**, 10965 (1992).
[8] The formation energy of a diluted defect is calculated at the equilibrium volume of the perfect crystal. See M. Finnis, *Interatomic Forces in Condensed Matter* (Oxford UP, Oxford, 2004), pp. 156-157.
[9] See e.g. M. Peressi, N. Binggeli, and A. Baldereschi, J. Phys. D: Appl. Phys. **31**, 1273 (1998). For cases with interface monopoles (absent in the present superlattice orientation) see F. Bernardini and V. Fiorentini, Phys. Rev. B **57**, R9427 (1998).
[10] V. Fiorentini, Phys. Rev. B **46**, 2086 (1992).
[11] F. Ricci, F. Boschi, A. Baraldi, M. Higashiwaki, A. Kuramata, A. Filippetti, V. Fiorentini, and R. Fornari, to be published.
[12] V. Fiorentini and A. Baldereschi, J. Phys.: Condens. Matter **4**, 5967 (1992); Phys. Rev. B **51**, 17196 (1995).